研究論文

A Close-up View of a Load Sensing "Hybrid" Proportional Directional Control Valve*

Gabriele ALTARE**, Damiano PADOVANI**, Nicola NERVEGNA**

The paper considers a stack of modular Load Sensing closed centre proportional directional control valves of a commercial excavator. All modules in the stack were disassembled and 3D models were prepared with the perspective of developing an accurate AMESim model. Previously, specific field measurements were also performed on the vehicle to set proper ground for subsequent validation of the simulation model. However, in the course of these in-depth investigations on all modules, some distinctive and rather peculiar aspects emerged. More precisely the pressure compensator featuring two independent spools, though located upstream of the main spool, is "normally" closed and in evident contrast with traditional pre-compensated solutions. In addition, the "global" Load Sensing signal driving the variable displacement pump differential pressure limiter is not originated by the highest load via proper selection in cascaded shuttle valves. The signal is rather generated by one of the two compensator spools through axial notches fed by a modest control flow directly derived from the pump delivery line. It is on this ground that, arbitrarily, due to their mixed origin, the term "hybrid" has been used in relation with these proportional directional control valves. The paper will detail all these findings and will further elucidate the AMESim model of one such modules. Finally simulated and experimental results will be contrasted to provide adequate support to the proposed modelling approach and a thorough analysis on specific parameters will be discussed.

Keywords: Spool Valve, Proportional Directional Control Valve, Flow Control, Simulation

1. Introduction

The majority of compact earth-moving machines presents mechanical-hydraulic Load Sensing (LS) circuits that, due to the complex working conditions that frequently involve multiple simultaneous functions, have to guarantee an independent velocity control of every user. This means to control the various flow rates (Q), expressed by Eq. (1) supplied to actuators through every proportional directional control valve (PDCV).

$$Q = C_e \cdot A(x) \cdot \sqrt{\frac{2 \cdot \Delta p}{\rho}} = k \cdot A(x) \cdot \sqrt{\Delta p} \qquad (1)$$

So, to decide every Q based only on operator's input (the main spool axial displacement x), it is necessary to keep the Δp across the metering area constant since other terms in Eq. (1) ideally comply with this requisite. As a consequence additional components are required and namely the local pressure compensators (LC). These items present two configurations (normally open or normally closed) and can be introduced in the circuit using various layouts: in general during simultaneous movements interactions among loads are avoided but proper control, when flow saturation occurs, is an aspect that only specific solutions can manage.

In fact pre-compensated solutions[1] (LCs located upstream the main spool and normally open) cannot work properly when flow saturation occurs, unless electronic control of the main spool position[2] is implemented, because the pump delivery pressure decreases so that the Δp across the highest load metering area is not constant at the reference value. On the contrary post-compensated solutions also known as "flow sharing" solutions[3,4,5] (LCs located downstream the main spool and normally closed) work with the same Δp across every metering area also during flow saturation so these Δps, though reduced with respect to the reference value, are nonetheless kept all equal.

However, there are other possibilities to realize pressure compensation in mechanical-hydraulic LS PDCVs. In particular, during an ongoing research on a hydraulic compact excavator, some distinctive aspects emerged concerning its LS PDCVs: in this context the term "hybrid" has been arbitrarily introduced since these components share concepts common to both previous categories (e.g. LCs located upstream the main spool but normally closed). So, aim of the present paper is to investigate and make clear the functioning of these components and provide an in-depth understanding of their behaviour by creating a virtual model and performing various simulation analyses.

*Manuscript received July 13, 2012
**Politecnico di Torino
(Corso Duca degli Abruzzi, 24, 10129 Torino, Italy)
E-mail: nicola.nervegna@polito.it

2. Nomenclature

A, B : load ports
C, D, E, F : hydraulic chambers
AC : anti-cavitation valve
AS : anti-shock valve
CV : check valve
DPL : differential pressure limiter
FGU : flow generation unit
LC : local pressure compensator
LS : load sensing
LSG : global load sensing
P : piston pump delivery port
P* : reduced pressure line
PDCV : proportional directional control valve
RV : relief valve
SP : spool
T : tank
TL : torque limiter
U : anti-shock line
UV : unloading valve
A : working area
$A(x)$: flow area
C_e : flow coefficient
F : force
f_S : force depending on a spring
k : constant value
p : generic hydraulic pressure
p^* : generic setting pressure
Q : flow rate
x : spool displacement
Δp : pressure difference
ρ : oil density

3. The considered compact excavator

3.1 A preamble on the machine

Nine users, split into two independent hydraulic circuits, can be activated by means of the PDCVs' stack installed on the machine and represented in Fig. 1. The LS circuit, supplied by a LS variable displacement pump, different from the original unit, feeds the boom, stick, bucket, right and left track motors, work tools and boom-swing, while the blade and the turret swing are part of the second circuit supplied by a fixed displacement gear pump. Displacement controls of specific interest in the present context are the DPL that maintains pressure p_P as expressed by Eq. (2) and a torque limiter TL.

$$p_P = p_{LSG} + p^*_{DPL} \quad (2)$$

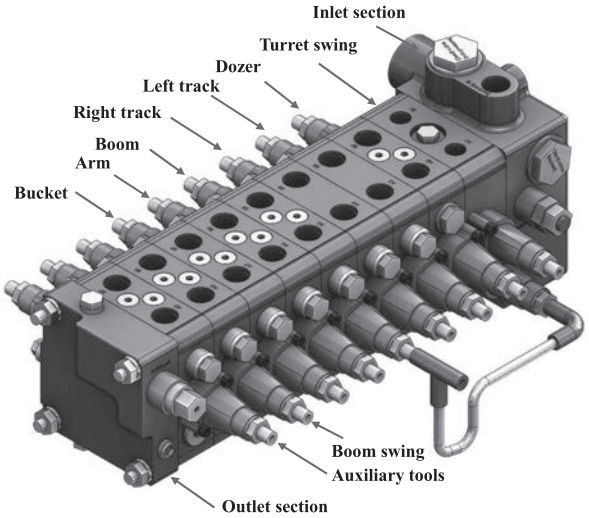

Fig. 1 Global view of the stack

The paper is focused on some LS components in the stack because of their particular structure concerning pressure compensation as well as LS signal selection [6]. Every LS PDCV is based on the same pressure compensation concept but some differences appear in the LS creation mode; in particular the two PDCVs dedicated to track users transfer the pressure signal from load port into the LS line, instead the other PDCVs create the LS signal throttling a modest control flow directly derived from the variable displacement pump delivery line. Owing to this particular arrangement, the topic is worthy of a thorough analysis.

3.2 The stack's structure

A preliminary step concerns the investigation of the stack's structure, so to evidence connections that affect every module.

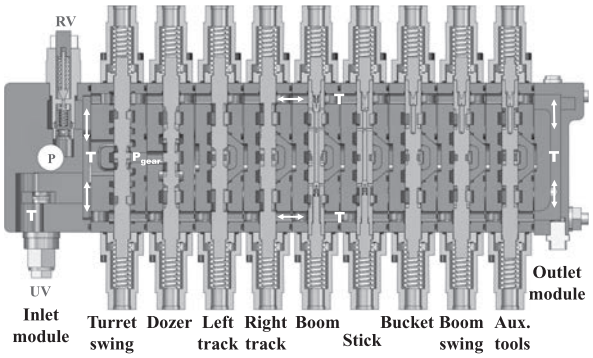

Fig. 2 Stack transversal section at main spools

Fig. 2 shows a transversal section of the PDCVs stack made at the mid-plane of the main spools where a ring shaped gallery collects all return lines to tank and a relief valve RV on the P port limits the maximum pump delivery pressure. Figure 3 shows a different section made at LCs mid-plane where a main gallery P and two pilot passageways

for p_P and p_{LSG} can be identified. An unloading valve UV is also visible that vents pump delivery pressure when p_{LSG} is null.

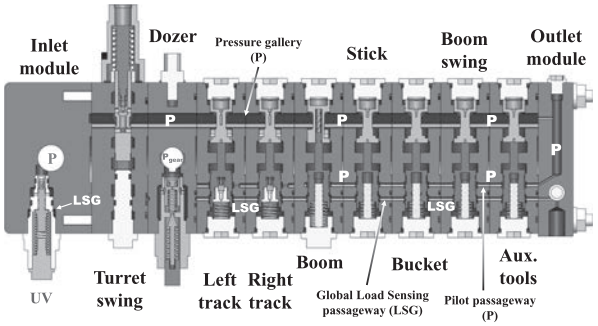

Fig. 3 Stack transversal section at LC spools

4. The Load Sensing PDCVs

4.1 An overview of a single component

The following analysis is referred to the boom-swing PDCV because it has no check valves inside its main spool to realize flow rate regeneration and its LC has the "basic" configuration among PDCVs in the stack, therefore a more general discussion can be covered; anyway other LS PDCVs have a similar structure.

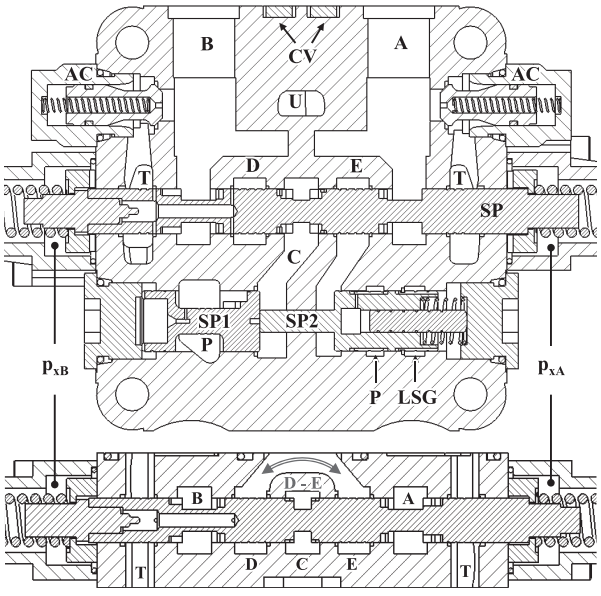

Fig. 4 Sections of the boom-swing PDCV

Connections among PDCVs modules and with the user can be seen in Fig. 4 that shows the longitudinal section at rest position (pilot stage controls of the main spool are only partially shown: all PDCVs' hydraulic pilot stages make use of a constant reduced pressure line P* derived from piston pump delivery P). In particular A and B are the load ports, P the piston pump delivery connections, LSG the global LS line connection, T the connections with tank and U is the connection with the anti-shock line. Inside this module the following components can be identified: the main spool (SP), the local pressure compensator spools (SP1 and SP2), two check valves (CV), and two anti-cavitation valves (AC). During working conditions the flow rate reaches chamber C located downstream spool SP1 and, if the main spool is displaced for instance to the left (p_{xA} is connected to the pressure reduced line P* and p_{xB} to tank), the flow reaches chamber D once throttled through the metering edges: thereafter channel D-E highlighted at the bottom of Fig. 4 (the channel is closed by the adjacent module) creates a connection with load port A. At the same time the flow rate discharged by the user's port B is returned to the tank line T.

On the contrary, if the main spool is displaced to the right (p_{xB} is connected to the pressure reduced line P*), load port B is supplied while load port A is discharged. Both CV valves connect every load port with the anti-shock line U that is common to nearly all modules in the stack (except track PDCVs) and ends with an anti-shock valve (AS) installed in the outlet module. CV valves select the highest pressure of all load ports and send it to the AS valve that has an equivalent pressure setting higher than the system relief valve (RV) setting. This solution has been developed to limit manufacturing costs because these CV valves are extremely simple and cheap while dual stage AS valves are certainly more expensive.

4.2 The PDCV's ISO scheme

The equivalent ISO scheme (Fig. 5), that presents the PDCV structure, is the starting point in analyzing the functioning of the component.

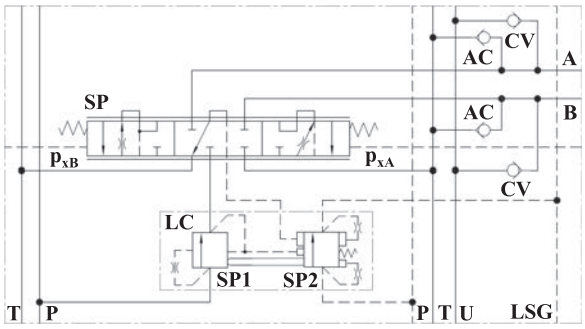

Fig. 5 ISO scheme of the boom-swing PDCV

Concerning LC's working areas (Fig. 6), spool SP1 has the same surfaces (A_1) on both extreme faces, while spool SP2 features a more complex geometry: in particular the stem of

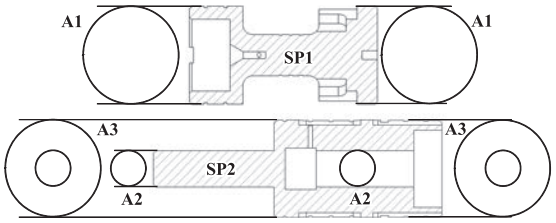

Fig. 6 Working areas of the LC's spools

SP2 creates a small surface (A_2) exposed to chamber C and an annulus surface (A_3) to chamber E. In addition spool SP2 houses a piston (it has the same diameter of the stem) that creates a small surface (A_2) exposed to chamber P and an annular surface (A_3) to LSG.

SP1 and SP2 spools work together, nevertheless they have different tasks: spool SP1 regulates the pressure upstream the metering area in addition to its check valve behaviour, while spool SP2 controls the LS signal generation (LSG) working as a pressure reducing valve that throttles a modest flow rate from P into LSG line; this line is always connected to tank by a bleed orifice (inserted into the outlet section).

Moreover spool SP2 also performs a hybrid shuttle valve function for the "selection" of the LS signals in each activated PDCV. Thus the presence of "real" shuttle valves is not necessary in the current configuration: this solution prevents drop of actuators that occurs in "conventional" LS circuits when the load pressure is transferred through the PDCV to the shuttle valve and then into the LSG line.

5. The PDCVs' functioning

At first, to understand the PDCVs' behaviour only one module is taken into consideration.

5.1 Rest position

At rest (Fig. 7) there are no pilot signals so the main spool stays spring centred. Chambers D-E are connected to tank through the main spool's radial-axial holes and the LSG signal

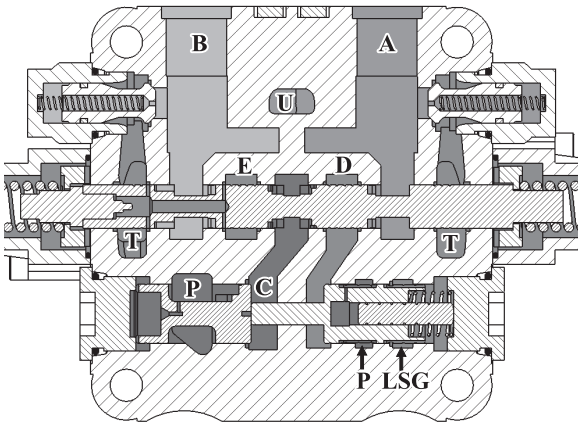

Fig. 7 Pressure distribution at rest position

is zero so pump delivery pressure is decided by the UV setting.

As a consequence different forces acting on LC keep spools in contact and displaced as in Fig. 7 (the real LC displacement at rest condition depends on clearances between spools and casing that also determine the transfer of pump delivery pressure into chamber C).

5.2 Transient

When a pilot signal is issued, for instance p_{xA}, the transient starts.

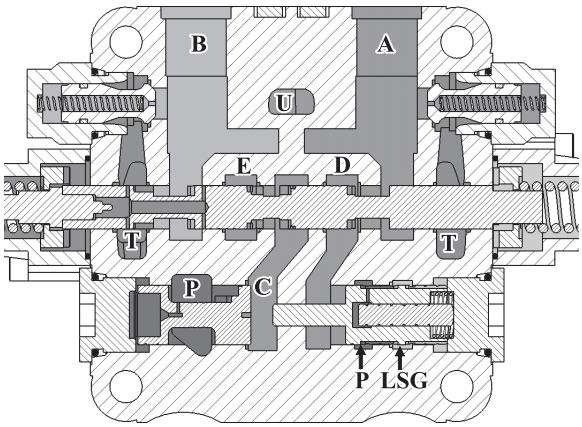

Fig. 8 General condition during transient

The new main spool position connects load port A with chambers D, E and C so load pressure (p_E) can act on surfaces A_3 and A_1 in chamber C: as a result spool SP1 moves to the left preventing backflow while spool SP2 shifts to the right connecting the pilot line P to the LSG line progressively increasing the LSG pressure level (Fig. 8).

Consequently the pump delivery pressure increases and this tendency continues until spools SP1 and SP2 can change position and move to come in contact: in this situation pressures in chamber E and in the LSG line are equal and the transient is ended.

5.3 Steady state condition (highest load)

At this stage both spools remain in contact and, under the hypothesis that only one user is active in the circuit, LC determines its spools' positions (Fig. 9) so to create the LS signal equal to the load pressure and transfer pump delivery pressure into chamber C.

However, if the user (a linear actuator) reaches an end-stop and the command on the PDCV persists LC spools separate.

5.4 Steady state condition (lower loads)

When multiple PDCVs are simultaneously active, each LC that controls a generic load with the exception of the highest behaves as displayed in Fig. 10.

The LSG line pressure is determined by the highest load

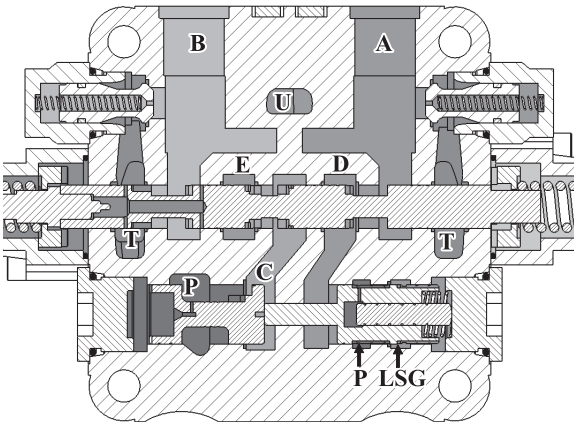

Fig. 9 Highest load condition when transient is finished

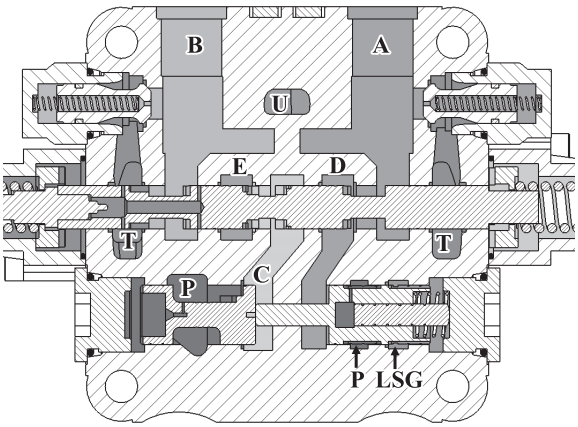

Fig. 10 Lower load condition when transient is finished

so the LC maintains its spools in contact. These shift so to regulate chamber C pressure that is now different from pump delivery pressure (this aspect will be detailed in the next paragraph).

5.5 The maintaining of Δp across metering edges

An important aspect concerns the evaluation of the Δp across the main spool metering area when LC is regulating and its spools are in contact. Figure 11 presents the equivalent ISO scheme of the boom-swing LC and provides the pertinent nomenclature. The equilibrium condition of spools SP1 and SP2 is described by Eq. (3).

$$\begin{cases} p_P \cdot A_1 = p_C \cdot A_1 + F \\ p_C \cdot A_2 + p_E \cdot A_3 + F = p_P \cdot A_2 + p_{LSG} \cdot A_3 + f_S \end{cases} \quad (3)$$

Considering spools in contact during LC steady state

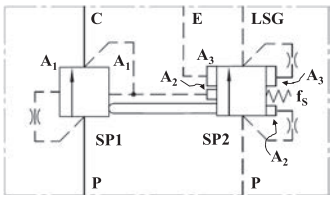

Fig. 11 ISO scheme of the boom-swing LC

regulating conditions, the mutually exchanged contact force (F) cancels, hence it is possible to write Eq. (4) where the last term is the equivalent pressure setting (p^*_{LC}) of the LC's spring.

$$p_C \cdot \frac{A_1 - A_2}{A_3} = p_P \cdot \frac{A_1 - A_2}{A_3} + p_E - p_{LSG} - \frac{f_S}{A_3} \quad (4)$$

Under the hypothesis that SP1 and SP2 have equal external diameters (as a consequence $A_1 - A_2 = A_3$), Eq. (4) becomes Eq. (5).

$$p_C = p_P + p_E - p_{LSG} + p^*_{LC} \quad (5)$$

Now, considering many PDCVs operating multiple functions simultaneously, every Δp across metering areas $A(x)$ is known. For the highest load ($p_E = p_{LSL} = p_{LSG}$) Eq. (6) can be written as:

$$\Delta p|_{A(x)} = p_C - p_E = p^*_{DPL} - p^*_{LC} \quad (6)$$

In this situation the Δp across the main spool metering area is constant so the flow rate directed to the actuator depends only on the flow area $A(x)$. For lower loads ($p_E = p_{LSL} < p_{LSG}$) Eq. (6) is still valid and the Δp across respective metering areas stays constant ("loads interference" does not take place).

5.6 Control of pump flow saturation

The analysed PDCV correctly handles pump flow saturation. For better comprehension, two users are considered with their PDCVs main spools so displaced to generate their maximum metering areas, one charged with the highest load (H) and the other with a lower load (L). Accordingly $p_{E,H} > p_{E,L}$. When flow saturation occurs, requested flow rates ($Q_R = Q_{RH} + Q_{RL}$) are in excess of pump flow rate (Q_P). The pressure drop $\Delta p'$ across the $PDCV_H$ metering area is lower than that existing on $PDCV_L$ still controlled by its LC. Hence, while user L receives Q_{RL} user H only profits of the remainder (Q_P - Q_{RL}) which is, in fact, lower than the desired Q_{RH}. At the same time pressure $p_{C,H}$ decreases inducing $SP1_H$ to move right determining the new pump delivery pressure (Eq. (2) is not valid anymore). Consequent to this pressure, $SP1_L$ moves left until force balance is re-established. Now from Eq. 5, the new $p_{C,L}$ can be determined and therefore the Δp across $PDCV_L$ is equal to $\Delta p'$. Therefore the total flow rate directed to users is equally shared between both.

5.7 SP1 and SP2 with different external diameter

SP1 and SP2 spools' external diameters are a design degree of freedom that can affect system behaviour (however SP2 external diameter is considered constant). If diameters are different, two cases take place. At first let us consider the situation where the surfaces' ratio introduced in Eq. (4) is greater than one (as a consequence $A_1 - A_2 > A_3$). The new Δp across the metering area is now described by relation (7),

neglecting the modest spring's force (p^*_{LC}).

$$p_C - p_E > p_P - p_{LSG} = p^*_{DPL} \quad (7)$$

This means that with the same load (p_E = const.) the attained Δp is higher than that associated with an areas ratio equal to one. Consequently, if x is the same, the flow rate directed to the actuator increases even though the load is constant: this difference is not too large but certainly represents an additional design opportunity for fine tuning control of the LS system. Conversely, if the opposite condition takes place (the surfaces' ratio is smaller than one, so $A_1 - A_2 < A_3$), equation (8) becomes valid: now the Δp across the metering area is lower and the actuator's velocity decreases.

$$p_C - p_E > p_P - p_{LSG} = p^*_{DPL} \quad (8)$$

6. A step forward

A thorough analysis on other PDCVs, such as that serving the bucket, brings to evidence a different design approach for SP2 and its piston (Fig. 12): the connection between chamber F and the LSG line occurs through an orifice O_F [7].

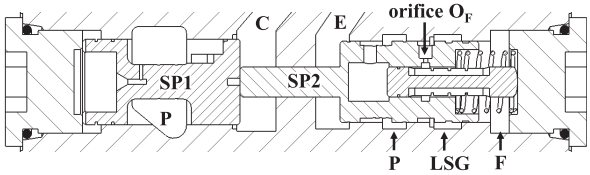

Fig. 12 Longitudinal section of the bucket LC

When multiple actuators are operated simultaneously, this solution avoids or at least limits actuators velocity reduction as soon as one of them reaches its end-stroke and the operator command still persists. In fact, without the orifice, p_F would coincide with p_{LSG} that, in turn, would reach the maximum pressure allowed by the RV; in this situation other LCs would be shifted left, limiting SP1 flow areas and therefore their respective flow rates.

Viceversa, the presence of orifice O_F uncouples p_F and p_{LSG} (it is discharging flow!) so that p_{LSG} cannot reach the maximum permitted value and its negative influence on other LCs' regulation is reduced (actuators can still move with the desired velocities).

7. The AMESim model of the bucket PDCV

In order to confirm the previous analysis, quantify some data and foresee the PDCV's behaviour by varying specific design parameters, the component has been modelled using AMESim (Fig. 13).

An extensive use of the HCD Library has been made: for instance the main spool presents a complex design with land notches as visible in Fig. 14 where plots of generated flow areas vs. spool displacement are also indicated.

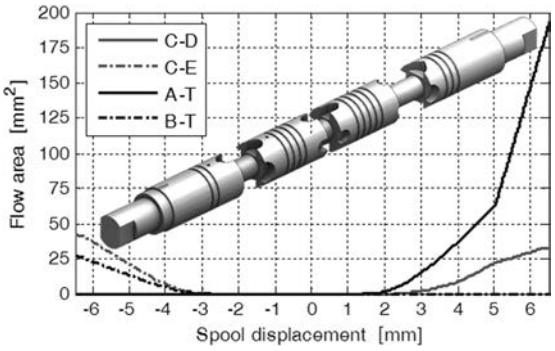

Fig. 14 Bucket PDCV's main spool geometry and flow areas

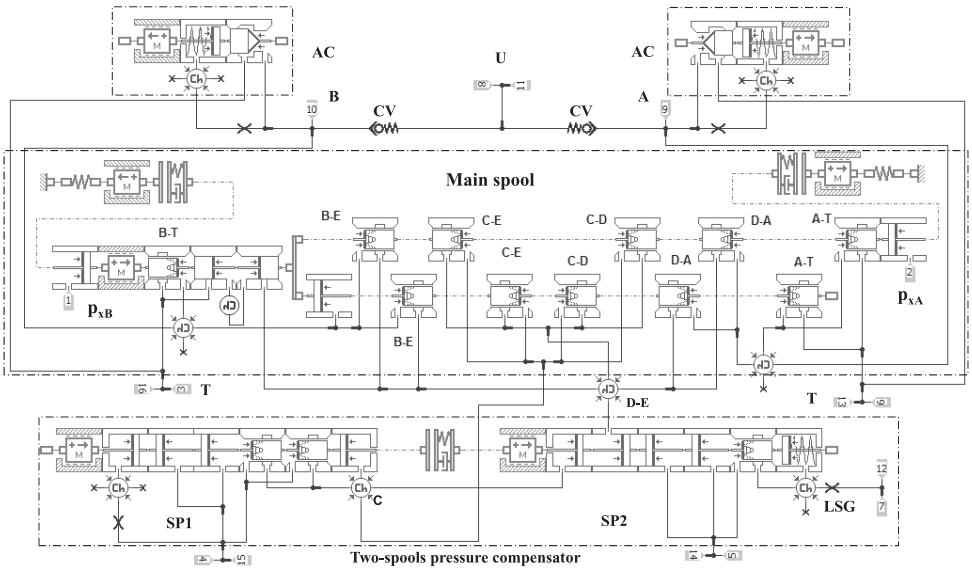

Fig. 13 AMESim sketch of the bucket PDCV

7.1 Model experimental validation

Tests conducted on the excavator allowed to acquire different data during the bucket test at various locations in the circuit, as indicated in Fig. 15.

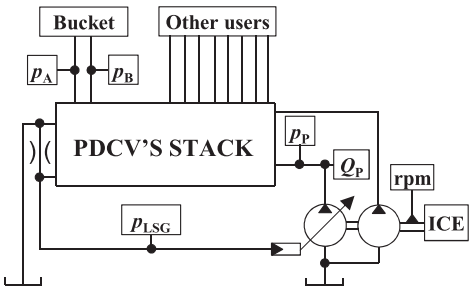

Fig. 15 Simplified machine layout with transducers positioning

7.2 Bucket closing and opening

This work cycle consists in the complete closing and opening of the bucket leaving other PDCVs at rest. Fig. 16 shows plots of pressures p_P and p_{LSG}, while in Fig. 17 pump flow rate is visible.

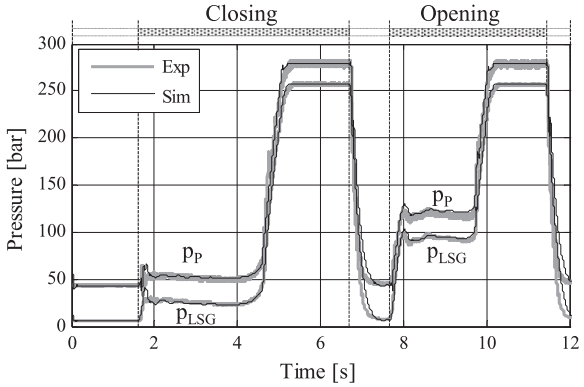

Fig. 16 Bucket test, p_P and p_{LSG} pressures

After a short initial delay (1.7 sec.) a command is issued aiming at the full closing of the bucket: the signal persists for a time period sufficient to complete this process and thereafter guarantee the intervention of the RV (4.6 sec.) in order to stabilize the system. The command ends (6.8 sec.) and then is so enacted (7.7 sec.) to feed the pump flow rate to the rod chamber of the bucket actuator. Also in this case the signal persists for a time period sufficient to complete bucket opening and grant pressure control through the RV (9.7 sec.). Due to hoses compliance, when the actuator reaches either end-stops, the pump flow rate quickly falls to about 20 L/min (conforming to the minimum swash plate angle). This minimum flow rate complements hoses expansion and thereafter both pressure and flow rate increase. While the former is limited by the RV (Fig. 16), the latter is instead bounded by the TL intervention (Fig. 17).

Pressures and flow rate comparisons indicate a good agreement between simulated and experimental results, though slight mismatches sometimes appear due to the simplifications introduced. For instance, since pump volumetric efficiency has only been measured at maximum displacement, experimental and simulated flow rates do not match exactly.

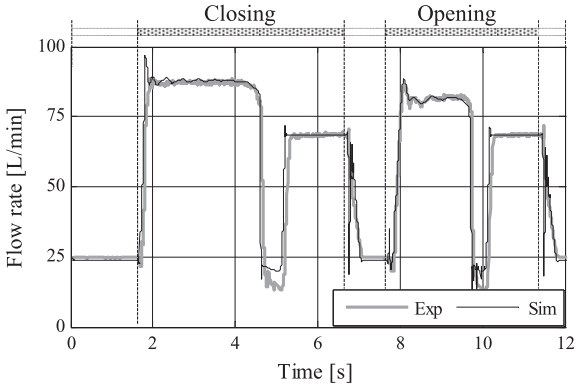

Fig. 17 Bucket test, piston pump flow rate

To confirm previous theoretical analyses and remarks, Fig. 18 supports aspects addressed in paragraph 5 concerning the LC behaviour.

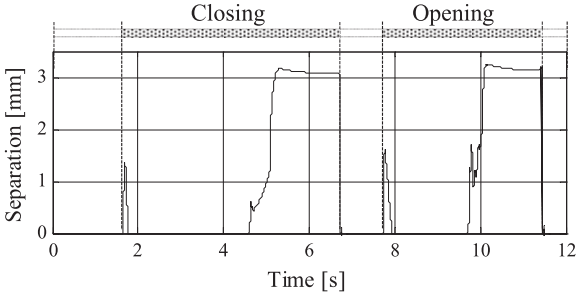

Fig. 18 Bucket test: separation between SP1 and SP2 spools

Separation between spools SP1 and SP2 is manifest during transients (around 1.7 and 7.7 sec.) and when the actuator reaches its end-stops (4.6 → 6.8 sec. and 9.7 → 11.5 sec). This does not happen when LC is regulating (1.8 → 4.6 sec. and 8 → 9.7 sec.).

In addition, with reference to paragraph 6, pressures in LC's chambers are shown in Fig. 19 where during bucket opening (7.5 → 9.7 sec.) p_E coincides with p_F while p_{LSG} is lower due to the influence of orifice O_F.

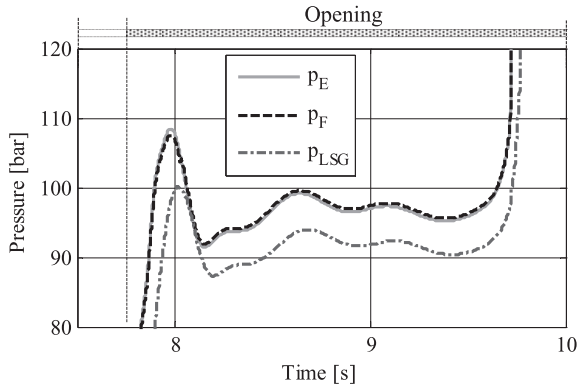

Fig. 19 Bucket opening: pressures p_E, p_F and p_{LSG}

8. Some virtual analyses

Simulations presented hereafter aim at scrutinizing the effects on system controllability consequent to the absence/presence of orifice O_F and to the adoption of different external diameters for the SP1 spools. To this purpose two PDCVs have been considered (Fig. 20) driving identical linear actuators charged with different and time varying loads (Load Act 1 < Load Act 2).

Non-dimensional commands shown in Fig. 21 on the two PDCVs are purposely conceived to evidence relevant system working phases: single movement (A), simultaneous movements (B), simultaneous movements in presence of flow saturation (C), single movement of actuator 2 consequent to actuator 1 reaching an end-stop (D). Commands time history determining main spools displacements has been kept the same for all investigations presented henceforth.

The torque limiter TL has been deliberately suppressed.

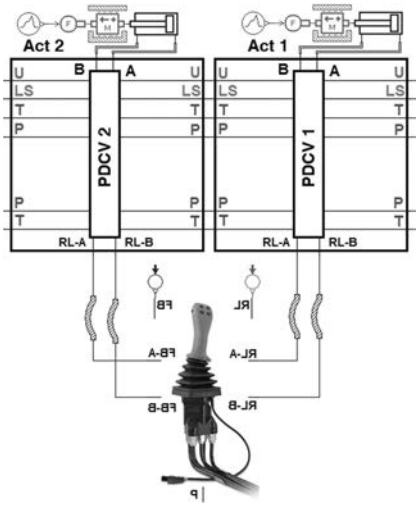

Fig. 20 AMESim sketch of the hydraulic system

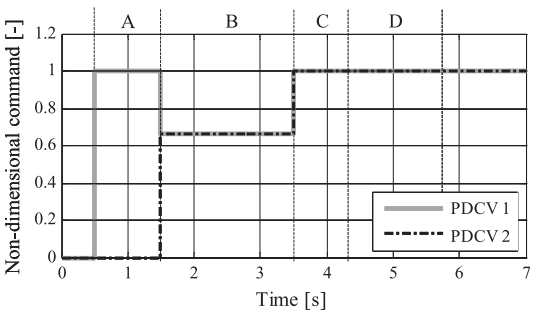

Fig. 21 Non-dimensional commands

8.1 Absence of orifice O_F in PDCVs

In this baseline system SP1 and SP2 have identical external diameters so that $A_1 - A_2 = A_3$. Fig. 22 (top) shows pressure drop Δp across PDCVs main spools, whereas correspondent actuators velocities and displacements are reported at the bottom.

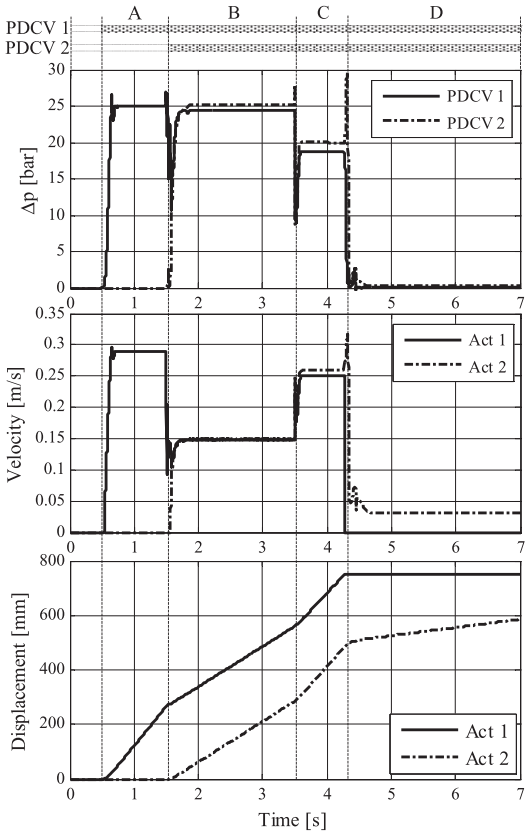

Fig. 22 Baseline system: Δp across metering areas, velocities and displacements

While only actuator 1 is moving (A phase) the Δp across the PDCV 1 metering area is 25 bar under control of the DPL.

From 1.5 sec. phase B begins and both PDCVs spools are positioned at an identically reduced travel (65%) so to avoid flow saturation. Despite different loading conditions the pressure drop on metering edges of both spools are quite close one another leading to practically identical actuators velocities. At about 3.5 sec. phase C is started where both spools are fully shifted (100%). The system is now facing flow

saturation (requested flow exceeds pump capacity) and the pressure drop Δp across spools metering edges is reduced. Consequently, actuators velocities though diminished remain constant during this phase thus preserving controllability.

The D phase starts when Act 1 reaches its end-stop (4.3 sec.) and its velocity falls to zero. Now the global LS signal p_{LSG} that was associated in previous phases with Act 2, is instead determined by Act 1 and is limited to about 270 bar by the RV. This bears a quite significant effect on the PDCV2 local compensator whose spools SP1 and SP2, in contact, become shifted to the left. Consequently, the Δp across the PDCV2 main spool metering edge drops sharply to less than 1 bar and Act 2 velocity becomes extremely low as Fig. 22 indicates. By evidence, in phase D controllability is lost. Changing the diameter of the two SP1 spools remedies this unacceptable behavior. For PDCV1 the baseline diameter was increased by 2.1 % while for PDCV2 the increase was 7.9 %.

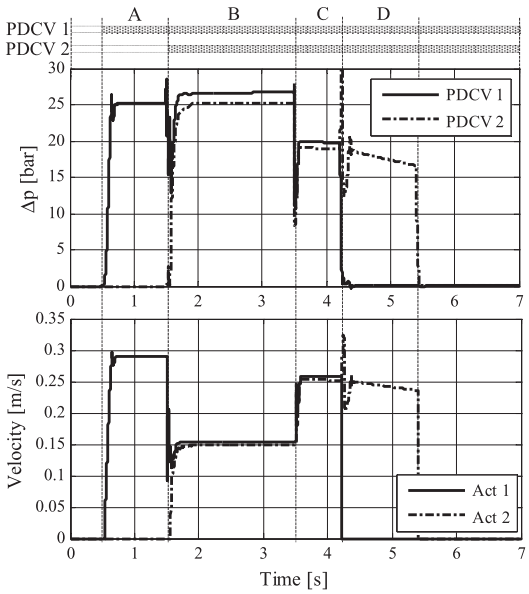

Fig. 23 Baseline system with SP1 different diameters

This intervention (Fig. 23) has almost negligible effects on the first three phases but is certainly beneficial in phase D where controllability of Act 2 is largely improved.

8.2 Presence of orifice O_F

The analysis is then extended in that the baseline configuration is again considered with the sole addition of orifices O_F in the two SP2 spools of local compensators (Fig. 24).

This is done to appraise consequences entailed by orifices O_F that, for higher load, uncouple p_{LSG} and p_F preserving the already existent proximity between p_E and p_F (see Fig. 25).

Fig. 26 shows that this leads to a system whose

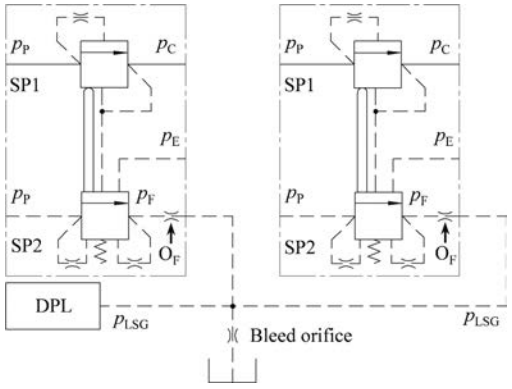

Fig. 24 Presence of orifice O_F

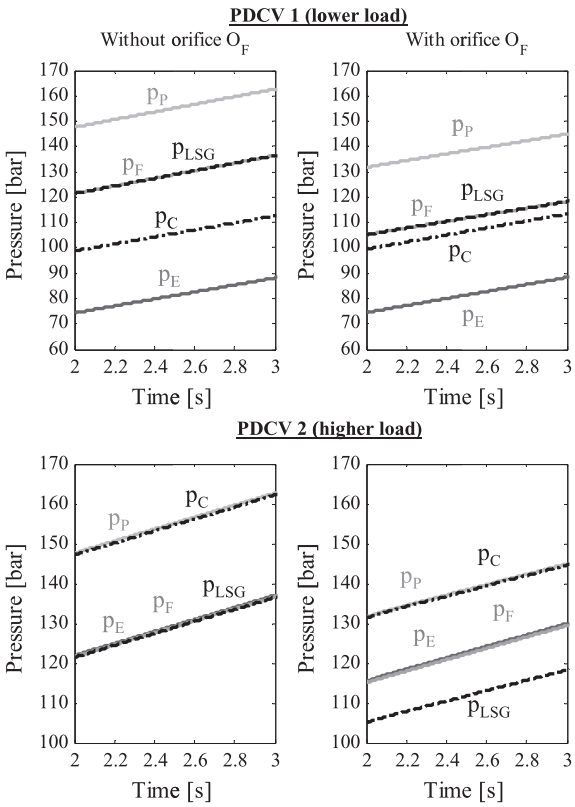

Fig. 25 Pressures inside a PDCV in phase A

controllability is clearly load dependent.

In fact, in phase A, as load increases, a noticeable difference is represented by a lower and linearly decreasing Δp across the PDCV 1 metering area (Fig. 26) with a concomitant velocity reduction.

Furthermore, phases B and C are adversely affected and specifically with respect to the higher loaded Act 2. Instead, in phase D the Δp across PDCV 2 metering area is slightly above 20 bar, so actuator 2 is now under control through the beneficial effect of the orifice. However, it should also be observed that going from phase C to phase D a sudden increase in PDCV 2 Δp causes an unpleasant increase in actuator's velocity. Thus, pro's and con's exist associated with

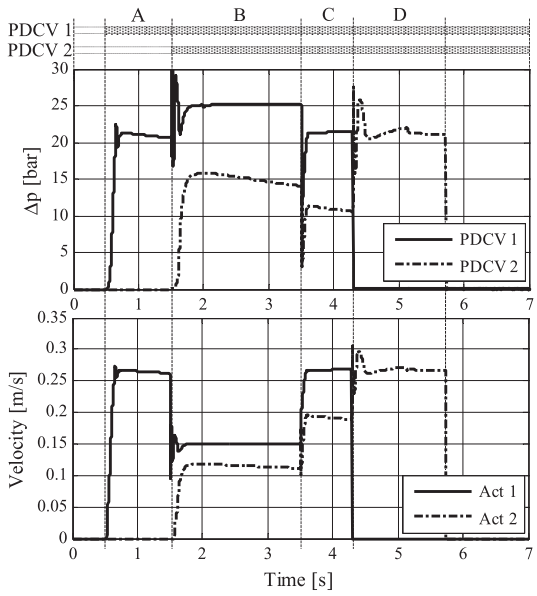

Fig. 26　Baseline system with orifice O_F

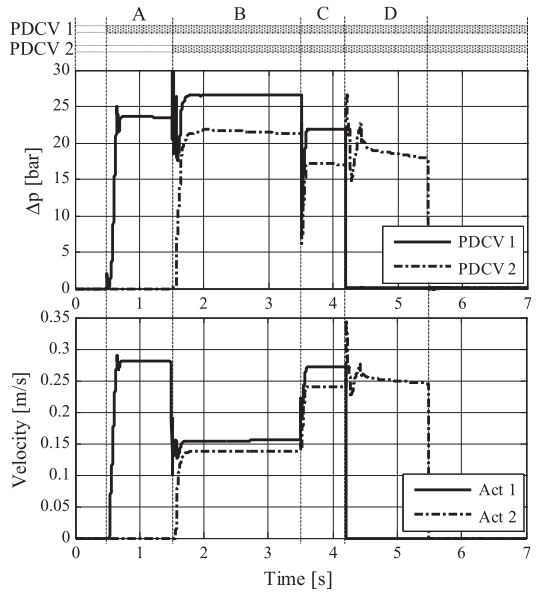

Fig. 27　Modified system

the adoption of orifice O_F.

Wishing to investigate further it was decided to act not only on the external diameters of the SP1 spools but also on the orifice diameters.

The baseline SP1 diameters were increased by 2.1% and 5.3% for the PDCV 1 and PDCV 2 respectively, while the orifice O_F was enlarged by 33%. Attained results are shown in Fig. 27 where a positive effect in terms of controllability is observed in all phases along with a mitigation relative to load dependency. There is no doubt that phase D is handled in a rather satisfactory way.

9. Conclusions

The present paper addressed some aspects of a "hybrid" PDCV of a commercial hydraulic excavator. Starting from a general description, the entire stack has been presented as well as modifications about the original layout of the hydraulic circuit. Afterwards, pressure compensation in these LS PDCVs has been analysed to show some peculiarities relative to the LS signal generation. The mathematical model of the PDCV has been presented and validated showing good agreement between experimental and simulated data. Virtual simulations were then performed to predict in contrast with a baseline configuration the influence on system controllability consequent to absence\presence of orifice O_F and to modifications of SP1 external diameter. The essential and distinct roles of these design variables have been clarified.

A more comprehensive study would have required an optimization approach that was however beyond the scope of the present research.

References

1）Zarotti, L. G., Nervegna, N., : Saturation Problems in Load Sensing Architectures, Proceedings of the National Conference on Fluid Power, 43rd Annual Meeting, Chicago, USA, p. 393-402, (1988).
2）LaFayette, G., Gruettert, S., Gandrud, M., Laudenbach, B., Koenemann, D.: Integration of Engine & Hydraulic Controls for Best Operation, 52nd National Conference on Fluid Power, Las Vegas, USA (2011).
3）Lantto, B., Palmberg, J.-O., Krus, P., : Static and Dynamic Performance of Mobile Load Sensing Systems with Two Different Types of Pressure - Compensated Valves, SAE Tech. paper No. 901552, (1990).
4）Rosenbecker, K., Chmielewski, C., : HUSCO's CompCheck® Technology – An Innovation Approach for Load Sensing Systems, SAE Tech. paper No. 932406, (1993).
5）Aoki, Y., Uehara, K., Hirose, K., Karakama, T., Morita, K., Akiyama, T., Oda, Y. : Load Sensing Fluid Power Systems, SAE Tech. paper No. 941714, (1994).
6）US Patent No. 5533334
7）US Patent No. 5735311